

EFFICIENT GRADIENT CALIBRATION BASED ON DIFFUSION MRI

Irvin Teh¹, Mahon L Maguire¹, and Jürgen E Schneider¹

¹Division of Cardiovascular Medicine, Radcliffe Department of Medicine, University of Oxford, Oxford, United Kingdom

Target Audience Scientists interested in the optimisation of diffusion MRI.

Purpose Accurate gradient calibration is a prerequisite for accurate diffusion MRI. Miscalibrated gradients can lead to systematic and magnified inaccuracies in measured diffusion metrics, eg. where the mean diffusivity depends on the square of the gradient amplitude. The corollary is that the measured diffusion has the potential to provide a simple and sensitive alternative to correction methods based on geometrical measurements. Here, we compared the measured diffusivity to that of a known reference at a given temperature, and generated corrections for the scaling terms for the three orthogonal gradients. The effect of the improvement in gradient calibration was assessed using diffusion tensor imaging (DTI) and anatomical imaging.

Methods A 20mm glass tube was filled with 99% cyclooctane (Sigma-Aldrich, MO, USA). A custom thermocouple (Harvard Apparatus, Kent, UK) secured to the surface of the tube recorded temperature at 1 Hz. MRI was performed using a 9.4T preclinical scanner (Agilent Technologies, Santa Clara, CA). A 3D echo planar imaging (EPI) sequence was used, where TR = 200 ms, TE = 12.5 ms, resolution = $375^3 \mu\text{m}$, $\delta = 3.5 \text{ ms}$, $\Delta = 7 \text{ ms}$, $b = [80, 320, 720, 1280, 2000] \text{ s/mm}^2$, acquisition time = 22m. The scan was non-slab-selective to minimise imaging gradients. Diffusion weighting (DW) and crushers were applied in the phase encoding direction only, eliminating off-diagonal b-matrix terms. Data were acquired in axial, coronal and sagittal orientations such that the DW was applied along the physical x, y, and z axes. The scan was first run with intentionally offset gradient scaling factors, Ψ_x, Ψ_y, Ψ_z . The measured diffusivity, D_m was calculated along the x, y, and z axes by fitting the data with a monoexponential decay. The mean temperature over each scan, T_m was determined for every acquisition. The reference diffusivity, D_r was calculated at T_m by fitting a 2nd-order polynomial to a range of reference diffusivity data¹. Gradient calibration factors, α_x, α_y and α_z were calculated using $\alpha = (D_r/D_m)^{0.5}$, and corrected scaling factors, Ψ'_x, Ψ'_y , and Ψ'_z were determined from $\Psi' = \alpha * \Psi$.

DTI was performed with a similar 3D EPI sequence (# B_0 images = 7, #DW directions = 30, $b = 2000 \text{ s/mm}^2$) before and after calibration, and the mean diffusivity (Mean D_m) and fractional anisotropy (FA) were measured in the phantom in the central five axial slices. Additionally, a custom-made phantom comprising two slotted orthogonal plates with a grid pattern of holes was built, and submerged in 0.5mM Gd solution. Gradient echo data with 100 μm isotropic resolution were acquired before and after calibration, and compared against reference 2D data acquired with a flatbed scanner at 5.3 μm isotropic resolution. Percent errors in distance from the central hole to the neighbouring holes in the positive x, y and z were measured.

Results We observed that the signal decay due to apparent diffusion, and hence D_m , increased with Ψ (Table 1). $D_m(x, y, z)$ were less variable with respect to each other post-calibration (Fig. 1) and approached D_r at given T_m (Table 1). The correction values derived were $\alpha_x = 1.083$, $\alpha_y = 1.030$ and $\alpha_z = 0.975$. The DTI results also show that the mean diffusivity post-calibration approached the reference mean diffusivity, while the FA was closer to zero, as would be expected in an isotropic phantom (Table 1). Errors in anatomical MRI were significantly reduced but not fully eliminated post-calibration (Fig. 2; Table 1).

Discussion We found that a major source of error in diffusion measurements could be attributed to the overall scaling of the x, y and z gradients. Rather than acquire new calibration data for each diffusion-weighted sequence^{2,3}, our modified method need only be performed once, is non-sequence-specific and improves both accuracy of diffusion and geometric measurements. Small residual errors in geometric measurements range from 40 to 265 μm , and could be improved by refining the semi-automated grid phantom measurements. The accuracy of the calibration does depend significantly on the accuracy and stability of the temperature measurements and the reference diffusivity data, and care has been taken to place the temperature probe close to the sample. In conclusion, we have demonstrated errors arising from inaccurate gradient calibration, and implemented a simple and efficient method for improving accuracy in diffusion and anatomical MRI.

References [1] Tofts P.S., et al. MRM. 2000; [2] Nagy Z., et al. MRM. 2007; [3] Teh I., et al. ISMRM. 2014. This work was supported by the EPSRC, UK (EP/J013250/1) and the British Heart Foundation (FS/11/50/29038).

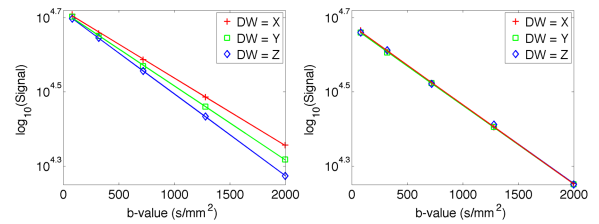


Figure 1. Log₁₀ of signal versus b-value pre-calibration (left) and post-calibration (right), R>0.999 for all fits.

	Pre-calibration	Post-calibration
$D_m(x)$ ($\times 10^{-4} \text{ mm}^2/\text{s}$)	4.23 ± 0.03	4.95 ± 0.04
$D_m(y)$ ($\times 10^{-4} \text{ mm}^2/\text{s}$)	4.65 ± 0.03	4.94 ± 0.03
$D_m(z)$ ($\times 10^{-4} \text{ mm}^2/\text{s}$)	5.08 ± 0.03	4.86 ± 0.03
$D_r(x)$ ($\times 10^{-4} \text{ mm}^2/\text{s}$)	4.96 ± 0.01	4.90 ± 0.07
$D_r(y)$ ($\times 10^{-4} \text{ mm}^2/\text{s}$)	4.93 ± 0.01	4.87 ± 0.05
$D_r(z)$ ($\times 10^{-4} \text{ mm}^2/\text{s}$)	4.82 ± 0.07	4.84 ± 0.02
Mean D_m ($\times 10^{-4} \text{ mm}^2/\text{s}$)	4.83 ± 0.38	4.97 ± 0.35
Mean D_r ($\times 10^{-4} \text{ mm}^2/\text{s}$)	4.93 ± 0.04	5.01 ± 0.01
FA	0.103 ± 0.011	0.032 ± 0.009
Error (x) (%)	-13.1	-5.3
Error (y) (%)	-5.0	-1.1
Error (z) (%)	1.9	-0.8

Table 1. Pre- and post-calibration measures of diffusion in cyclooctane phantom and geometric accuracy in grid phantom.

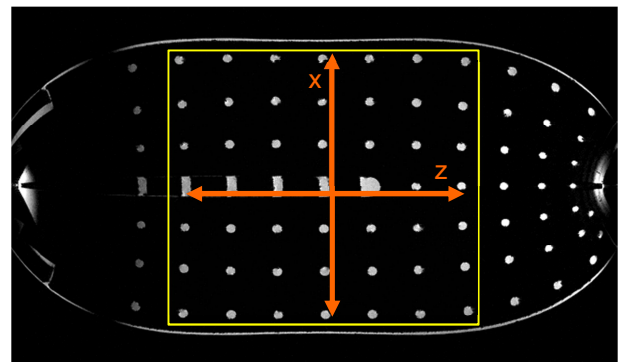


Figure 2. Gradient echo image of grid phantom in coronal orientation. Orthogonal plate in sagittal plane not shown.